Clamping of ferroelectric and antiferromagnetic order parameters of $YMnO_3$

2003 J. Phys.: Condens. Matter 15 L103

(http://iopscience.iop.org/0953-8984/15/3/102)

INSTITUTE OF PHYSICS PUBLISHING JOURNAL OF PHYSICS: CONDENSED MATTER

J. Phys.: Condens. Matter **15** (2003) L103–L109 PII: S0953-8984(03)56269-5

LETTER TO THE EDITOR

Clamping of ferroelectric and antiferromagnetic order parameters of $YMnO_3$

Eiichi Hanamura[1,4], **Katsumi Hagita**[2] **and Yukito Tanabe**[3]

[1] Chitose Institute of Science and Technology, 758-65 Bibi, Chitose, Hokkaido 066-8655, Japan
[2] Japan Science and Technology Corporation (CREST), 758-65 Bibi, Chitose, Hokkaido 066-8655, Japan
[3] Department of Applied Physics, University of Tokyo, 7-3-1 Hongo, Bunkyo-ku, Tokyo 113-8656, Japan

E-mail: hanamura@photon.chitose.ac.jp

Received 19 November 2002
Published 13 January 2003
Online at stacks.iop.org/JPhysCM/15/L103

Abstract

It was observed that a ferroelectric domain boundary (DB) is always accompanied by an antiferromagnetic DB in hexagonal $YMnO_3$, by means of interference effects of the second-harmonic signal. The clamping of these two order parameters at the ferroelectric DB is shown theoretically to originate from Dzyaloshinski–Moriya interaction. This interaction favouring a right angle between the neighbouring spins is found to be operative within the DB and to reverse the direction of the spins across the ferroelectric DB.

The theoretical and experimental studies of ferroelectromagnets—crystals with magnetic and ferroelectric (FEL) orderings—were reviewed by Smolenskii and Chupis [1]. There are very few natural multiferroic magnetoelectrics that are both ferromagnetic and ferroelectric in the same phase. The fundamental physics behind the scarcity of coexistence of ferromagnetism and ferroelectricity was discussed recently by Hill [2]. On the other hand, there are many ferroelectric antiferromagnets (AFM), e.g., hexagonal rare-earth manganites $RMnO_3$(R = Sc, Y, In, Ho–Lu) with smaller radius of the ion R^{3+} than in perovskite manganites [3]. It has been commonly accepted [1], on the grounds of the Ginzburg–Landau (GL) theory based on the bulk free energy, that there will be only weak coupling between the FEL and AFM order parameters in the case where the critical temperatures T_C and T_N are greatly different. This is indeed the case for $YMnO_3$ with $T_C = 914$ K and $T_N = 74$ K. Anomalies in the dielectric constant and loss tangent of this crystal were observed at T_N but these anomalies are small, reflecting the weak coupling [4, 5].

Optical second-harmonic spectroscopy has proved to be a powerful means for determination of complex magnetic structures—for example, the noncollinear AFM structure

[4] Author to whom any correspondence should be addressed.

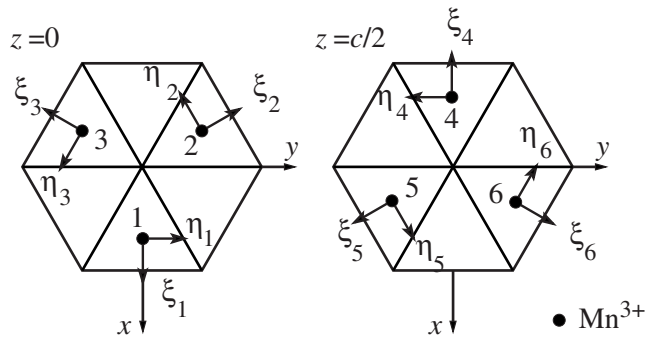

Figure 1. Six Mn ions in the unit cell and the local axis. The oxygens are located at the centre and each corner. The distance between the nearest-neighbouring oxygens is denoted as $\rho \equiv a/\sqrt{3}$ with the lattice constant a.

of the hexagonal manganites [6, 7]. This type of second-harmonic generation (SHG) can be described mainly in terms of the time-covariant susceptibility $\chi^{(c)}_{yyy}(2\omega)$ and the time-invariant one $\chi^{(i)}_{zyy}(2\omega)$. The nonlinear susceptibility $\chi^{(c)}_{yyy}(2\omega)$ is found [8, 9] to be proportional to the product of the FEL $\langle P_z \rangle$ and the AFM $\langle S_x \rangle$ order parameters and its peak is located at $2\hbar\omega = E(^5\mathrm{E}_1\mathrm{b}) = 2.45$ eV, while $\chi^{(i)}_{zyy}(2\omega)$ is linearly proportional to $\langle P_z \rangle$ with its peak at $E(^5\mathrm{E}_1\mathrm{a}) = 2.7$ eV in $YMnO_3$. Here the first subscript y or z denotes the polarization of the SHG signal and the second and third ones those of the fundamental wave.

Making use of these characteristics, we can observe four kinds of domain of FEL AFM, i.e., (++), (−−), (+−), and (−+) [9]. The first sign here stands for the FEL polarization $\langle P_z \rangle$, while the second one denotes the sublattice magnetization $\langle S_x \rangle$ of the Mn1 ion in figure 1, i.e., the order parameter of the AFM domain. It is noted here that the six sublattice magnetizations in the unit cell in figure 1 are transformed into each other by symmetry operations of $P6'_3/cm'$, so that the AFM order can be described in terms of $\langle S_x \rangle$ for the Mn1 ion. We can distinguish (a) the FEL domain boundary (DB) by observing the external interference of the SHG described by $\chi^{(i)}_{zyy}$ with the SHG signal from quartz, (b) the product pattern of $\langle P_z \rangle$ and $\langle S_x \rangle$ by observing the external interference of the SHG described by $\chi^{(c)}_{yyy}$ also with the quartz signal, and (c) the AFM domains by observing the internal interference of the SHG signals described by $\chi^{(i)}_{zyy}$ and $\chi^{(c)}_{yyy}$. It has been found that the FEL DB is always accompanied by the reversal of the sublattice magnetization $\langle S_x \rangle$, in agreement with the clamping model [8, 9]. This means that the (++) domain is preferentially in contact with the reversed FEL domain (−−) and not with (−+) or (+−), while the (−+) domain is in contact with the (+−) domain and not with (++) or (−−), i.e., that the two order parameters $\langle P_z \rangle$ and $\langle S_x \rangle$ are strongly coupled at the FEL DB.

The coupling of two order parameters is a topic of general interest, discussed among physicists in general in terms of the GL equation. The coupling of two order parameters induced at the DB is quite a new concept. Recently some efforts have been made to control the magnetic order by applying an electric field or, conversely, to control the electric order by means of a magnetic field [10]. Here the coupling of two order parameters plays an important role. Application of the FEL property of $YMnO_3$ in nonvolatile memory was proposed [11]. In erasing or rewriting such memories, motion of these DBs is inevitable. In the present letter, we will propose a microscopic mechanism of clamping of FEL and AFM DBs in $YMnO_3$, which will be found to be induced by the Dzyaloshinski–Moriya (DM) interaction [12, 13].

We will consider a spatially inhomogeneous plate of a FEL AFM in equilibrium. The splitting of such a material into FEL domains is shown to be accompanied also by an

inhomogeneous distribution of the AFM vector. A hexagonal $YMnO_3$ crystal shows a uniaxial ferroelectricity $\langle P_z \rangle = P$ with six sublattice magnetizations. The exchange interaction of Mn^{3+} spins is described as a sum of an isotropic and an antisymmetric anisotropic term as follows:

$$\mathcal{H} = -2\sum_{\langle i,j \rangle} J_{ij} \boldsymbol{S}_i \cdot \boldsymbol{S}_j + \sum_{\langle i,j \rangle} d_{ij} (\boldsymbol{S}_i \times \boldsymbol{S}_j)_z, \tag{1}$$

where $-2J_{ij}$ is the superexchange interaction between the nearest-neighbour Mn^{3+} ions $\langle i, j \rangle$ and d_{ij} is the DM term arising from the exchange interaction modified by the spin–orbit interaction $\mathcal{H}_{so} = \lambda \sum_i \boldsymbol{L}_i \cdot \boldsymbol{S}_i$ and the lower-symmetry crystalline field V_{zx} [8].

We treat our spin system in the continuum approximation [14]. In this approximation, we set

$$\boldsymbol{S}_2(\boldsymbol{r}_1 + \boldsymbol{\rho}_{12}) = \boldsymbol{S}_2(\boldsymbol{r}_1) + \boldsymbol{\rho}_{12} \cdot \nabla \boldsymbol{S}_2 + \tfrac{1}{2}(\boldsymbol{\rho}_{12} \cdot \nabla)^2 \boldsymbol{S}_2 + \cdots \tag{2}$$

for the spin of Mn2 nearest to Mn1 at $\boldsymbol{r}_1$. Here $\boldsymbol{\rho}_{12}$ is a vector drawn from Mn1 pointing to the nearest-neighbour Mn2.

The interlayer superexchange interaction is smaller by more than an order of magnitude than the intralayer one [8]. Therefore the exchange interaction energy is evaluated within one layer, say $z = 0$, neglecting the interlayer interaction and confining the spins within the ab-plane. The AFM state consists of triangular sublattice magnetization in each ξ_i $(i = 1, 2, 3)$ direction and the spin system is well described by classical vectors [15, 16]: $\langle S_{i\xi} \rangle = S \cos \phi_i$ and $\langle S_{i\eta} \rangle = S \sin \phi_i$ for the Mn ions $(i = 1, 2, 3)$ in the $z = 0$ plane with $S = 2$. Here ϕ_i is measured from $\theta_1 = 0$, $\theta_2 = 2\pi/3 \equiv \theta$, and $\theta_3 = -2\pi/3$ for three Mn ions in the $z = 0$ plane. Let us assume that $\theta = 2\pi/3 \gg |\phi_i - \phi_j|$ for any pair i and j, and set $\phi_1 = \phi_2 = \phi_3 = \phi$. Hereafter we choose the FEL and AFM DBs perpendicular to the y-axis and assume both P and ϕ to depend on only the y-coordinate, i.e., $P \equiv P(y)$ and $\phi \equiv \phi(y)$. For this FEL DB, the exchange energy, which comes from the first term of equation (1) and is dependent on the rotation angle ϕ, is derived in the continuum approximation as

$$E_{exch}(\phi) = -\frac{a^2}{\Omega} 3|J| \cos\theta S^2 \int \mathrm{d}x\, \mathrm{d}y\, \frac{1}{2}\left(\frac{\mathrm{d}\phi}{\mathrm{d}y}\right)^2. \tag{3}$$

Here the superexchange interaction via the oxygen ion is denoted as $-2J (J < 0)$. The unit-cell area Ω is equal to $\sqrt{3}/2a^2$, and θ is $2\pi/3$, i.e., the angle between two composite spins of the neighbouring Mn^{3+} ions. Similarly, the anisotropy energy is evaluated as

$$E_{anis}(\phi) = -\frac{1}{\Omega} \int \mathrm{d}x\, \mathrm{d}y\, 3(D + E) S^2 \cos^2 \phi. \tag{4}$$

The constant term was disregarded in equation (4). Here $D + E = 3\lambda^2/E_2 - 3\lambda^2/E_1$ with $E_2 = E(^5\mathrm{E_1b}) - E(^5\mathrm{A_1}) = 2.45$ eV and $E_1 = E(^5\mathrm{E_1a}) - E(^5\mathrm{A_1}) = 2.7$ eV. We have neglected the change of J and $D + E$ within the FEL DB. The DM interaction, which is effective within one layer and is given by the second term of equation (1), is transformed into the following form:

$$E_{DM}(\phi) = \frac{1}{\Omega} \int \mathrm{d}x\, \mathrm{d}y\, D_y(\boldsymbol{r}) S^2 \cos\theta \frac{\mathrm{d}\phi}{\mathrm{d}y}, \tag{5}$$

with

$$D_y(\boldsymbol{r}) = \tfrac{1}{2} \sum_{(ijk)} \sum_{\rho} \{(\boldsymbol{\rho}_{ij})_y d_i(\boldsymbol{r}, \boldsymbol{r} + \boldsymbol{\rho}_{ij}) + (\boldsymbol{\rho}_{ik})_y d_i(\boldsymbol{r}, \boldsymbol{r} + \boldsymbol{\rho}_{ik})\}. \tag{6}$$

Here $\sum_{(ijk)}$ stands for the summation over cyclic changes of the subscripts i, j, and k, and $d_{ij} \equiv d_i(\boldsymbol{r}, \boldsymbol{r} + \boldsymbol{\rho}_{ij})$ is derived as

$$d_{ij} = 2\lambda\left[\frac{J_{ij}(20,00)}{E_1E_2}V_i - \frac{J_{ij}(00,20)}{E_1E_2}V_j\right], \tag{7}$$

where $\langle\Psi_0|V(z\xi)|\Psi_1\rangle_i \equiv V_i$, $\langle\Psi_1|\mathcal{H}_{so}|\Psi_2\rangle_i = -\mathrm{i}\lambda S_{iz}$ [8], and the off-diagonal superexchange is defined by

$$\langle\Psi_2\Psi_0|\mathcal{H}_{ex}|\Psi_0\Psi_0\rangle_{ij} \equiv -2J_{ij}(20,00)\boldsymbol{S}_i \cdot \boldsymbol{S}_j, \tag{8}$$

$$\langle\Psi_0\Psi_2|\mathcal{H}_{ex}|\Psi_0\Psi_0\rangle_{ij} \equiv -2J_{ij}(00,20)\boldsymbol{S}_i \cdot \boldsymbol{S}_j. \tag{9}$$

We may assume V_i and V_j are proportional to P. Then, we can set

$$d_{ij} = a_{ij}P + b_{ij}\,\mathrm{d}P/\mathrm{d}y \tag{10}$$

in the region where P is a function of the coordinate y, with the constant coefficients a_{ij} and b_{ij}. The second term in equation (10) corresponds to the difference between V_i and V_j. When we choose the origin of the coordinate y at the middle of the FEL boundary region, we find that $P(y)$ is an odd function of y, while the derivatives $\mathrm{d}P/\mathrm{d}y$ and $\mathrm{d}\phi/\mathrm{d}y$ are even functions. This implies that we are allowed to keep only the term proportional to $\mathrm{d}P/\mathrm{d}y$ in D_y and set

$$D_y = \lambda_0\,\mathrm{d}P/\mathrm{d}y, \tag{11}$$

with a proportionality constant λ_0 in the integrand of equation (5). It is also noted that the magnetic structure is not affected in the uniform system by the DM interaction given by the second term of equation (1).

For the FEL and AFM DBs perpendicular to the y-axis, the free energy density f of $P(y)$ and $\phi(y)$ is described as follows:

$$f = f_P + f_\phi + f_{P\phi}, \tag{12}$$

where

$$f_P = \frac{1}{2}\alpha_3\left(\frac{\mathrm{d}P}{\mathrm{d}y}\right)^2 - \frac{1}{2}\alpha_1P^2 + \frac{1}{4}\alpha_2P^4, \tag{13}$$

$$f_\phi = \frac{1}{2}\beta_2\left(\frac{\mathrm{d}\phi}{\mathrm{d}y}\right)^2 - \frac{1}{2}\beta_1\cos^2\phi, \tag{14}$$

$$f_{P\phi} = \lambda''\left(\frac{\mathrm{d}P}{\mathrm{d}y}\right)\left(\frac{\mathrm{d}\phi}{\mathrm{d}y}\right). \tag{15}$$

Here $\beta_1 = 6(D+E)S^2/\Omega$, $\beta_2 = 3a^2|J|S^2/2\Omega$, and $\lambda'' = -\lambda_0S^2/2$. From the calculation of the variations for $I_P \equiv \int f_P(y)\,\mathrm{d}x\,\mathrm{d}y$, the function $P(y)$ should obey the following equation:

$$\alpha_3\frac{\mathrm{d}^2P}{\mathrm{d}y^2} - \alpha_2P^3 + \alpha_1P = 0. \tag{16}$$

Although a more general solution of equation (16) may be given in terms of elliptic functions [17], we choose a single DB solution:

$$P(y) = P_0\tanh(y/\delta_P) \tag{17}$$

with

$$P_0 = \sqrt{\alpha_1/\alpha_2} \qquad \text{and} \qquad \delta_P = \sqrt{2\alpha_3/\alpha_1}. \tag{18}$$

The DB of the sublattice magnetization $\phi(y)$ is also similarly obtained from equation (14) as a solution of the following equation [18]:

$$\beta_2\frac{\mathrm{d}^2\phi}{\mathrm{d}y^2} = \frac{1}{2}\beta_1\sin 2\phi. \tag{19}$$

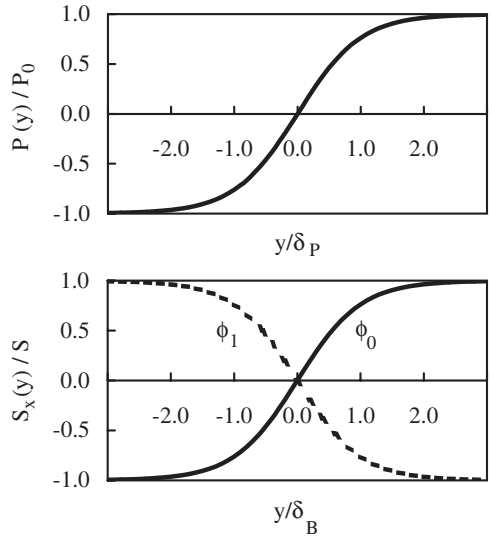

Figure 2. Spatial dependences of the order parameters of (a) the ferroelectricity $P(y)$ and (b) the sublattice magnetization $S_x(y)$. Solid and dotted curves show, respectively, $S\cos\phi_0$ and $S\cos\phi_1$.

The boundary conditions $\mathrm{d}\phi/\mathrm{d}y = 0$ at $y = \pm\infty$ are also derived at the same time. The solution of equation (19), which is nothing but the sine–Gordon equation of the present day, has been fully discussed [19]. The solution which starts from the value $\phi = \pi$, i.e., $S_x = -S$ at $y = -\infty$, decreases around $y = 0$, and tends to $\phi = 0$ ($S_x = S$) at $y = \infty$ is given by

$$\phi_0 = \begin{cases} \pi - \sin^{-1}\left(\operatorname{sech}\dfrac{y}{\delta_B}\right) & \text{for } y < 0, \\ \sin^{-1}\left(\operatorname{sech}\dfrac{y}{\delta_B}\right) & \text{for } y > 0, \end{cases} \tag{20}$$

where the Bloch wall width δ_B is given by $\delta_B = \sqrt{\beta_2/\beta_1}$. Solutions of equations (17) and (20) describe the DB $(--) \leftrightarrow (++)$ as shown in figure 2. The DB $(-+) \leftrightarrow (+-)$ is described by

$$\phi_1 = \begin{cases} -\sin^{-1}\left(\operatorname{sech}\dfrac{y}{\delta_B}\right) & \text{for } y < 0, \\ -\pi + \sin^{-1}\left(\operatorname{sech}\dfrac{y}{\delta_B}\right) & \text{for } y > 0. \end{cases} \tag{21}$$

The structures of these Bloch walls and FEL DBs are shown in figure 2. Remember that $S_x(y) = S\cos\phi(y) = \pm S\tanh(y/\delta_B)$.

Here the nonlocal bilinear coupling equation (5) of the two order parameters due to the DM interaction is shown to contribute to the clamping of the two order parameters, because the solution equations (20) and (21) give the same stability energy:

$$E_{DM} = L_x \int_{-\infty}^{\infty} \mathrm{d}y\, \lambda'' P_0 \frac{1}{\delta_P} \operatorname{sech}^2\left(\frac{y}{\delta_P}\right)\left(-\frac{1}{\delta_B}\right)\operatorname{sech}\left(\frac{y}{\delta_B}\right), \tag{22}$$

with L_x the length of the unit cell in the x-direction when $\lambda'' P_0 > 0$. We may interchange the first and the second lines in equations (20) and (21) for the opposite case $\lambda'' P_0 < 0$. This also gives the clamping of the two order parameters. The stability energy E_{DM} depends weakly on the relative value δ_B/δ_P of the wall widths; e.g., $E_{DM} = -\pi I_0$ for $\delta_B \ll \delta_P$,

$E_{DM} = -\pi I_0/2$ for $\delta_B = \delta_P$, and $E_{DM} = -2I_0\delta_P/\delta_B$ for $\delta_B \gg \delta_P$, with $I_0 = L_x\lambda'' P_0/\delta_P$. We can show mathematically that the homogeneous solution of equation (19), $\phi = 0$ (with no AFM domain wall), is prohibited around the FEL DB. The FEL DB is much stronger than the AFM exchange and anisotropy energies. Therefore the exact equation of motion for ϕ is derived from equation (12) with the spatially fixed FEL DB as

$$\beta_2 \frac{\mathrm{d}^2\phi}{\mathrm{d}y^2} = \frac{1}{2}\beta_1 \sin 2\phi - \lambda'' \frac{\mathrm{d}^2 P}{\mathrm{d}y^2}. \tag{23}$$

The solution $\phi = 0$ is shown to be unstable, so it is not allowed in the presence of the antisymmetric term (the second term on the right-hand side in equation (23)) due to the FEL DB. Note that equation (19) is an approximate form of equation (23) and the effect of this antisymmetric term has been evaluated as a perturbation as in equation (22). This means that the FEL DB should always be accompanied by an AFM DB.

We shall estimate the numerical values of relevant physical quantities by setting the spin–orbit interaction $\lambda \sim 10$ meV, the superexchange interaction $|J| \sim 17$ meV [20], and the crystalline field $V(z\xi) \sim 0.6$ eV [8]:

$$E_{exch}(\phi) = 120(L_x/\delta_B)\ \text{meV}, \tag{24}$$

$$E_{anis}(\phi) - E_{anis}(\phi = 0) = 0.28\left(\frac{L_x\delta_B}{a^2}\right)\ \text{meV}, \tag{25}$$

$$E_{DM}(\phi) = -0.24\left(\frac{L_x}{a}\frac{\delta_P}{\delta_B}\right)\ \text{meV}. \tag{26}$$

We can also evaluate the Bloch wall width $\delta_B = \sqrt{\beta_2/\beta_1} \sim 20\ a$, but no information is available for the magnitude of δ_P. However, we expect δ_P to be much smaller than δ_B, under which assumption equation (26) was obtained.

The stability energy due to the clamping of the FEL and AFM DBs perpendicular to the x-axis is shown to vanish. Therefore we may expect anisotropy of these DBs. The FEL DB, however, even with just a small component along the x-axis, should always be clamped with an AFM DB due to the DM interaction. In conclusion, we have theoretically confirmed that the FEL DB is always accompanied by reversal of the sublattice magnetization in hexagonal $YMnO_3$, while the AFM DB may exist by itself. This looks consistent with the observed result. There remaining two problems for the future. First, the extension to the three-dimensional GL model [21] is an interesting problem relating to the phenomenon considered here. Second, the magnetoelastic effect in which the exchange interaction is modified by the lattice distortion at the FEL DB may be related to the present model [22]; clarification of this relationship is required.

Useful discussions with N Nagaosa, Y Tokura and M Fiebig are appreciated.

References

[1] Smolenskii G A and Chupis I E 1983 *Sov. Phys.–Usp.* **25** 475
[2] Hill N A 2000 *J. Phys. Chem.* B **104** 6694
[3] See, e.g.,
van Aken B 2002 *Proefschrift* Rijksuniversiteit Groningen (and references therein)
[4] Huang Z J, Chao Y, Sun Y Y, Xue Y Y and Chu C W 1997 *Phys. Rev.* B **56** 2623
[5] Katsufuji T, Mori S, Masaki M, Moritomo Y, Yamamoto N and Takagi H 2001 *Phys. Rev.* B **64** 104419
[6] Fröhlich D, Leute St, Pavlov V V and Pisarev R V 1998 *Phys. Rev. Lett.* **81** 3239
[7] Fiebig M, Fröhlich D, Kohn K, Leute St, Lottermoser Th, Pavlov V V and Pisarev R V 2000 *Phys. Rev. Lett.* **84** 5620

[8] Iizuka-Sakano T, Hanamura E and Tanabe Y 2001 *J. Phys.: Condens. Matter* **13** 3031
[9] Fiebig M *et al* 2002 *Nature* **419** 818
[10] Tokura Y 2002 *Workshop on Phase Control of Correlated Electron Systems (Waikola, HI, May 2002)*
[11] Fujimura M, Ishida T, Yoshimura Y and Ito T 1996 *Appl. Phys. Lett.* **69** 1011
[12] Dzyaloshinski I 1958 *J. Phys. Chem. Solids* **4** 241
[13] Moriya T 1960 *Phys. Rev. Lett.* **4** 228
[14] Herring C and Kittel C 1951 *Phys. Rev.* **81** 869
[15] Kittel C 1949 *Rev. Mod. Phys.* **21** 541
[16] Pananicolaou N 1995 *Phys. Rev.* **51** 15062
[17] Soboleva T K and Stefanovskii E P 1983 *Sov. Phys.–Solid State* **25** 1637
[18] Bloch F 1932 *Z. Phys.* **24** 195
[19] See, e.g.,
Dodd R K, Eilbeck J C, Gibbon J D and Morris H C 1982 *Solitons and Nonlinear Wave Equations* (New York: Academic)
[20] Takahashi J, Hagita K, Kohn K, Tanabe Y and Hanamura E 2002 *Phys. Rev. Lett.* **89** 76404
[21] Winternitz P, Grundland A M and Tuszynski J A 1988 *J. Phys. C: Solid State Phys.* **21** 4931
[22] Gaididei Yu B, Saxena A, Lookman T, Bishop A R and Büttner H 2002 *Phys. Rev.* **66** 140403